JOURNAL OF PETROLOGY | VOLUME 42 | NUMBER 7 | PAGES 1387–1400 | 2001

Sr, Nd, Pb and O Isotopes of Minettes from Schirmacher Oasis, East Antarctica: a Case of Mantle Metasomatism involving Subducted Continental Material

MARION HOCH[1]*, MARK REHKÄMPER[2,3] AND HEINZ J. TOBSCHALL[1]

[1]INSTITUTE OF GEOLOGY AND MINERALOGY, UNIVERSITY OF ERLANGEN–NÜRNBERG, SCHLOSSGARTEN 5, D-91054 ERLANGEN, GERMANY

[2]INSTITUTE OF MINERALOGY, UNIVERSITY OF MÜNSTER, CORRENSSTR. 24, D-48149 MÜNSTER, GERMANY

[3]INSTITUTE OF ISOTOPE GEOLOGY AND MINERAL RESOURCES, ETH ZURICH, NO C61, CH-8092 ZÜRICH, SWITZERLAND

RECEIVED OCTOBER 7, 1999; REVISED TYPESCRIPT ACCEPTED NOVEMBER 15, 2000

Numerous minette dykes intersect the Precambrian crystalline basement of Schirmacher Oasis, East Antarctica. This study presents new Sr, Nd, Pb and O isotope data for 11 minette samples from four different dykes. The samples are characterized by relatively high $^{87}Sr/^{86}Sr$ *(0·7077–0·7134),* $^{207}Pb/^{204}Pb$ *(15·45–15·55) and* $^{208}Pb/^{204}Pb$ *(37·8–39·8), combined with low* $^{143}Nd/^{144}Nd$ *(*$\varepsilon_{Nd} = -6{\cdot}5$ *to* $-25{\cdot}1$*) and variable* $^{206}Pb/^{204}Pb$ *(16·8–18·1). The* $\delta^{18}O$ *values are high, ranging from* $+6{\cdot}5$ *to* $+9{\cdot}5$‰ *SMOW. Rb/Sr whole-rock–biotite isochrons suggest an age of* ∼*455 Ma for emplacement of the minette dykes. The major and compatible element geochemistry of the minettes indicates derivation of the magmas from a mantle source. The enriched isotopic and trace element signatures of the dykes cannot be due to contamination of the ascending magmas by continental crust. Rather, the geochemical characteristics of the minettes are most reasonably explained by partial melting of a lithospheric mantle source that was enriched by metasomatic fluids derived from recycled continental crust. If mantle enrichment took place just before dyke emplacement, the isotopic systematics of the minettes must be inherited directly from the metasomatic agents, and this would indicate derivation of the fluids from recycled lower continental crust.*

KEY WORDS: *Antarctica; isotopes; mantle metasomatism; minettes, lithospheric mantle*

INTRODUCTION

Minette magmas are generally thought to represent small-degree melts that form at depths of ∼50–150 km within the lithospheric mantle. The deep origin of such lamprophyric magmas is indicated by entrained mantle xenoliths of spinel peridotite or garnet peridotite composition, and the geochemistry of the magmas (e.g. Rogers *et al.*, 1982; Stille *et al.*, 1989; Wyman & Kerrich, 1993; Carlson & Irving, 1994; Carmichael *et al.*, 1996). Minettes typically display intermediate to basic compositions with high contents of MgO, Cr and Ni, and high *mg*-number. Additionally, however, minettes are also characterized by high concentrations of large ion lithophile elements (LILE), particularly Ba, Sr and Rb, and they are enriched in light rare earth elements (LREE). Thus minettes display high abundances of both compatible and highly incompatible trace elements. This requires the involvement of at least two distinct source components for the generation of minette magmas: (1) a peridotitic mantle reservoir and (2) a component enriched in LILE and LREE. It is conceivable that the enrichment of incompatible trace elements results from the contamination of the magmas with crustal materials during dyke emplacement. Alternatively, a number of studies have indicated that

*Corresponding author. Telephone: 0049-9131-852-2660. Fax: 0049-9131-852-9294. E-mail: mhoch@geol.uni-erlangen.de

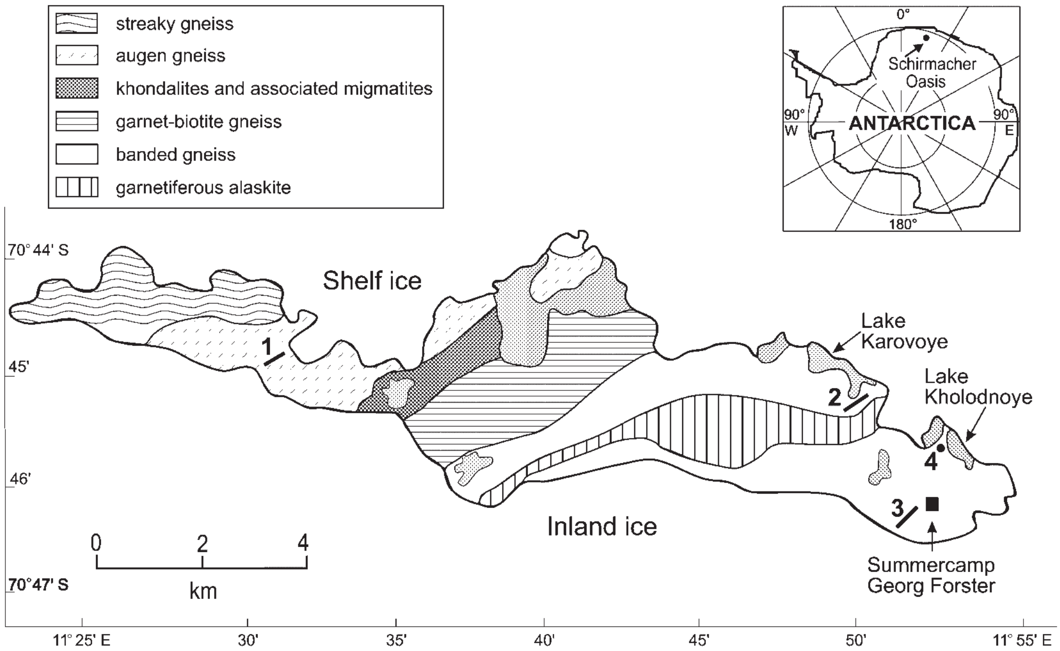

Fig. 1. Schematic geological map of the Schirmacher Oasis, East Antarctica, and location of the minette dykes analysed in this study (after Sengupta, 1988). Dyke 1: samples N7 (margin) to N10 (centre), thickness 1–2 m; Dyke 2: samples 268 (margin) to 270 (centre), thickness 1·2 m; Dyke 3: samples L6/1 (margin) to L6/4 (centre), thickness 1·3 m; Dyke 4: sample Oa3.

minettes are derived from enriched lithospheric reservoirs. It has been suggested that such reservoirs are formed by the interaction of refractory peridotitic material with a metasomatic component released from subducted continental material in a collision or subduction zone setting (e.g. Nelson, 1992; Stern & Hanson, 1992; Carmichael *et al.*, 1996; Becker *et al.*, 1999).

This study presents new Sr, Nd, Pb and O isotope compositions for 11 representative minette samples from the Schirmacher Oasis, East Antarctica. The new results are used to constrain the age of the lamprophyre dykes and the origin of the incompatible element-enriched signatures of the minettes. These minette samples are of particular interest in this respect, because a previous trace element study indicated that the mantle source of the magmas may have been metasomatically modified by fluids or melts released from subducted sediments (Hoch & Tobschall, 1998).

SAMPLES

The Schirmacher Oasis is located near the Princess Astrid Coast, Central Queen Maud Land, East Antarctica at 70°44′–70°47′S, 11°25′–11°55′E (Fig. 1). This ice-free area of ~35 km^2 extends nearly parallel to the east–west-trending coastline and is situated approximately halfway between the coastal ice shelf and the main mountain range of Queen Maud Land. The crystalline basement of the Schirmacher Oasis forms part of the East Antarctic craton (Sengupta, 1991; Paech & Stackebrandt, 1995). The geology is dominated by six major rock sequences, which consist mainly of different gneiss varieties (Fig. 1). Numerous dykes of lamprophyre, basalt, dolerite, pegmatite and aplite intruded into this poly-metamorphic complex.

Eleven minettes from four dykes were analysed in the present study. The samples were collected in 1983–1984 by H. Kämpf and U. Wand (now at GeoForschungsZentrum Potsdam) during the 29th Soviet Scientific Expedition to Queen Maud Land, East Antarctica. Sample locations are shown in Fig. 1. The minette dykes trend predominantly ENE–WSW, with a dip of 50–85° NNW or 40–70° SSE, and they are between 0·5 and 3 m wide. The studied samples are invariably porphyritic with panidiomorphic texture, containing mafic megacrysts (biotite > amphibole and/or pyroxene) in a feldspar groundmass (K-feldspar > plagioclase). Detailed petrographic investigations indicate that all samples are fairly fresh, with only minor signs of greenschist alteration (Hoch, 1997).

ANALYTICAL METHODS

For the analyses of whole-rock samples, 100–200 mg of powder were digested with $HF–HNO_3–HClO_4$ and HCl.

Pure mineral separates of biotite (100 mg) were hand-picked under a binocular microscope from a split of coarsely crushed whole-rock powder. Standard chromatographic techniques were applied for the separation of Rb–Sr, Sm–Nd and U–Pb from the rock samples. Total chemistry blanks were <2·0 ng for Rb, <300 pg for Sr, <300 pg for Nd, <30 pg for Sm, <50 pg for Pb, and <16 pg for U, and are thus insignificant.

Radiogenic isotope compositions were measured at the Mineralogisch–Petrographisches Institut, Universität München (Sr, Nd), and the Institut für Geowissenschaften und Lithosphärenforschung, Universität Gießen (Pb), by thermal ionization mass spectrometry (TIMS) using a Finnigan MAT 261 instrument. The concentrations of the elements Rb, Sr, Nd, Sm, U and Pb were determined by isotope dilution-TIMS. Fractionation corrections, isotopic standard values and the external precision of the measurements are reported in the captions of Tables 2–4 (below). The oxygen isotope analyses were performed on whole-rock samples following extraction of oxygen using purified fluorine and subsequent conversion into CO_2. The measurements were made on a PRISM I mass spectrometer (VG Instruments) at the Mineralogisch–Petrographisches Institut, Universität Bonn. All results are reported relative to Standard Mean Ocean Water (SMOW) in the common δ-notation. The overall reproducibility of $\delta^{18}O$ values averaged $\pm 0{\cdot}1$‰ (1σ).

RESULTS

Major and trace elements

The major and trace element geochemistry of the Schirmacher minettes has been discussed in detail in a previous publication (Hoch & Tobschall, 1998) and only a brief summary is given here. The minettes are characterized by an intermediate to basic composition with *mg*-number ranging from 57 to 74, and MgO contents of 5·1–11·6% (Table 1). In most cases, the compositional differences among samples of the same dyke are significantly smaller than the overall range in chemical compositions (Table 1). Plots of SiO_2, Al_2O_3, Cr and Ni vs *mg*-number indicate that fractional crystallization of olivine and pyroxene occurred during magma evolution (Hoch & Tobschall, 1998). Not all minette samples follow a single liquid line of descent and this suggests that the dykes are derived from different parental magmas. Further characteristics of the samples are the high contents of volatiles and alkali elements, as well as the high abundances of Ni and Cr, particularly in the least evolved samples of each dyke (Table 1).

All minettes are characterized by high concentrations of LILE, particularly Rb, Ba, Th, K and LREE (Table 1, Fig. 2). The incompatible trace element abundances range from ~10 (Ti, Y) to 1000 (Ba) times primitive mantle values. Positive spikes in the trace element patterns are particularly apparent for Ba and Rb (and, in many samples, Pb), whereas Nb and Ti display negative anomalies (Fig. 2). As a result of these systematics, the minettes are characterized by low Nb/U (10·5 ± 5·2) and Nd/Pb (3·7 ± 2·5) ratios.

Rb–Sr isochron ages

The $^{87}Rb/^{86}Sr$ ratios of minette samples from the same dyke display only very limited variation. To obtain precise age information, it was thus necessary to analyse hand-picked biotite mineral separates from each dyke (Table 2). Isochron ages were then calculated for the dykes, by combining the biotite data with the whole-rock results for samples from the same dyke (Tables 2 and 3). Identical formation ages of 445·5 ± 9·8 Ma and 445·8 ± 4·5 Ma were obtained for Dykes 1 and 2, respectively, whereas Dyke 3 was dated at 728 ± 13 Ma (Table 2).

There exists only a very limited number of previous geochronological studies on rocks of the Schirmacher Oasis and lithostratigrapic correlations with other metamorphic complexes in Queen Maud Land are still of uncertain significance (Paech & Stackebrandt, 1995). Grew & Manton (1983) reported U–Pb ages for allanites and zircons from gneisses of the Schirmacher Hills with upper and lower concordia intercept ages of 1500 Ma and 630 Ma, respectively. The 1500 Ma age was interpreted to represent a primary deformation event under high-grade (granulite-facies) conditions. The lower-intercept age probably marks the subsequent re-equilibration of the rocks under amphibolite-facies conditions. Ravich & Soloviev (1966) documented maximum K/Ar ages of 845–830 Ma for mafic granulites from the Schirmacher Oasis. Most ages for rocks and minerals from the Schirmacher Oasis, however, are younger at ~700–500 Ma (Ravich & Krylov, 1964; Grew & Manton, 1983; Kämpf & Stackebrandt, 1985), probably as a result of the pervasive reactivation of this crustal segment during the Pan-African orogeny (Bormann *et al.*, 1995; Paech & Stackebrandt, 1995).

The basement rocks of the Schirmacher Oasis are intersected by numerous lamprophyre, basalt, pegmatite and aplite dykes, and few of these intrusions have been the subject of geochronological investigations. Conventional K/Ar dating of whole-rock samples shows two age-groups for the basalts—Palaeozoic and Mesozoic (Kaiser & Wand, 1985; Wand *et al.*, 1988). The only data existing for pegmatites from this region are Pb/Pb model ages of between 865 and 600 Ma for K-feldspars (Bielicki *et al.*, 1991). Field observations indicate that the lamprophyres from the Schirmacher Oasis are older than the basalts, but younger than the pegmatites (Paech & Stackebrandt,

Table 1: Concentrations of selected major and trace elements in the Schirmacher minettes (Hoch & Tobschall, 1998)

Dyke no.:	1	1	1	2	2	2	3	3	3	3	4
Sample:	N7	N9	N10	268	269	270	L6/1	L6/2	L6/3	L6/4	Oa3
wt %											
SiO_2	53·6	51·6	51·1	51·6	49·6	49·9	51·4	52·4	52·2	52·8	55·4
Al_2O_3	14·17	12·45	11·46	13·38	12·07	12·74	11·26	11·62	11·45	11·91	12·02
Fe_2O_3 (t)	7·67	8·83	9·01	7·58	9·04	7·85	7·88	7·64	7·75	7·49	7·67
MgO	5·12	6·56	8·70	7·75	11·12	9·17	11·58	10·12	10·60	9·56	8·11
CaO	6·06	6·89	7·40	5·91	6·03	7·03	5·25	5·59	5·46	5·40	5·65
K_2O	5·68	5·83	5·19	4·67	4·68	4·83	6·10	6·21	6·10	6·26	5·33
H_2O^+	0·82	1·04	1·07	1·36	1·96	1·66	1·96	1·73	1·57	1·85	1·66
mg-no.	56·9	59·5	65·7	66·9	70·9	69·8	74·4	72·3	73·1	71·6	67·7
ppm											
Cr	198	465	803	307	632	452	637	604	586	582	390
Ni	44	70	115	160	295	194	88	73	79	61	92
Ba	5460	5910	4740	6180	4570	6620	3850	4120	4030	4030	7430
Th	23	18	16	16	13	14	11	12	12	12	16
Nb	13	21	18	15	32	32	16	12	12	15	23
Zr	409	401	385	328	323	342	410	421	416	426	510
La	90·9	80·7	74·9	106	91·2	126	57·8	68·4	65·7	68·5	104
Yb	2·51	2·45	2·26	2·46	2·04	2·41	2·07	2·23	2·17	2·30	2·81

mg-number = 100 × molar Mg/(Mg + Fe*); Fe* is total Fe calculated as FeO (Rudnick, 1995).

Table 2: Rb and Sr concentrations and Sr isotope ratios of biotites, and whole-rock–biotite isochron ages of the Schirmacher minette dykes

	Biotite N10 Dyke 1	Biotite 269 Dyke 2	Biotite L6/1 Dyke 3
Rb (ppm)	534	373	240
Sr (ppm)	35·1	148	98
$^{87}Rb/^{86}Sr$	43·62	7·06	6·88
$^{87}Sr/^{86}Sr \pm 2\sigma_{mean}$	0·986548 ± 25	0·752144 ± 23	0·776562 ± 26
Dyke age (Ma)	445·5 ± 9·8*	445·8 ± 4·5†	728 ± 13‡
MSWD	82	1·6	17
$(^{87}Sr/^{86}Sr)_i$	0·70971 ± 58	0·70729 ± 3	0·70507 ± 18

The Rb–Sr isochrons of the dykes and associated MSWD values were calculated with Isoplot/Ex Version 2·01 (Ludwig, 1999).
*Isochron includes biotite N10 and samples N7, N9 and N10.
†Isochron includes biotite 269 and samples 268–270.
‡Isochron includes biotite L6/1 and samples L6/1–L6/4.

1995). Dayal & Hussain (1997) obtained Rb/Sr whole-rock–mineral isochron ages of 455 ± 12 Ma and 458 ± 6 Ma for two lamprophyre dykes from the Schirmacher Oasis.

It is noteworthy that the latter results are very similar to the 446–445 Ma ages that were obtained for the minettes of Dykes 1 and 2 in the present study. The ~730 Ma age that was obtained for Dyke 3, however,

Table 3: Rb and Sr concentrations, Sr isotope ratios and initial $^{87}Sr/^{86}Sr$ values of the Schirmacher minettes

Sample	Rb (ppm)	Sr (ppm)	$^{87}Rb/^{86}Sr$	$^{87}Sr/^{86}Sr \pm 2\sigma_{mean}$	$(^{87}Sr/^{86}Sr)_i$
N7	180	933	0·5387	0·712875 ± 11	0·70946
N9	150	1283	0·3264	0·711967 ± 10	0·70990
N10	184	944	0·5443	0·713238 ± 8	0·70978
268	127	2209	0·1605	0·708332 ± 11	0·70731
269	143	1841	0·2168	0·708638 ± 14	0·70726
270	149	1981	0·2099	0·708628 ± 11	0·70729
L6/1	157	1320	0·3320	0·708369 ± 12	0·70626
L6/2	142	1596	0·2483	0·707745 ± 14	0·70617
L6/3	147	1552	0·2643	0·707863 ± 9	0·70619
L6/4	149	1541	0·2698	0·707858 ± 10	0·70615
Oa3	190	1064	0·4986	0·713373 ± 10	0·71021

$^{87}Sr/^{86}Sr$ ratios are normalized to $^{86}Sr/^{88}Sr = 0{\cdot}1194$ and are reported relative to $^{87}Sr/^{86}Sr = 0{\cdot}71023$ for NIST-987 Sr. Repeated standard measurements ($n = 32$) indicate an external reproducibility (2σ) of 0·006%. For samples N7–N10 and 268–270, the initial isotopic ratios were calculated with the whole-rock–biotite isochron ages of the corresponding dykes (Table 1). For samples Oa3 and L6/1–L6/4 the initial values were calculated for an age of 445 Ma (see text).

Table 4: Nd and Sm concentrations, Nd isotope ratios, initial $^{143}Nd/^{144}Nd$ values, ε_{Nd} and Nd model ages of the Schirmacher minettes

Sample	Nd (ppm)	Sm (ppm)	$^{147}Sm/^{144}Nd$	$^{143}Nd/^{144}Nd \pm 2\sigma_{mean}$	$(^{143}Nd/^{144}Nd)_i$	ε_{Nd}	$\varepsilon_{Nd(t)}$	$T_{(DM)}$(Ga)
N7	66·25	11·07	0·1031	0·511644 ± 5	0·51134	−19·4	−14	2·0
N9	79·30	13·58	0·1057	0·511584 ± 9	0·51128	−20·6	−15	2·1
N10	65·11	11·10	0·1052	0·511618 ± 7	0·51131	−19·9	−15	2·1
268	93·43	15·31	0·1010	0·511810 ± 7	0·51151	−16·2	−11	1·7
269	110·15	18·20	0·1020	0·511792 ± 7	0·51149	−16·5	−11	1·8
270	115·06	18·63	0·0999	0·511802 ± 6	0·51151	−16·3	−11	1·7
L6/1	75·73	17·04	0·1389	0·512307 ± 8	0·51190	−6·5	−3	1·6
L6/2	83·99	18·29	0·1344	0·512269 ± 8	0·51188	−7·2	−3	1·6
L6/3	80·37	17·50	0·1344	0·512293 ± 4	0·51190	−6·7	−3	1·5
L6/4	81·66	18·99	0·1436	0·512291 ± 7	0·51187	−6·8	−4	1·7
Oa3	94·82	16·67	0·1085	0·511353 ± 13	0·51104	−25·1	−20	2·5

$^{143}Nd/^{144}Nd$ ratios are normalized to $^{146}Nd/^{144}Nd = 0{\cdot}7219$ and are reported relative to $^{143}Nd/^{144}Nd = 0{\cdot}511755$ for MERCK-Nd and $^{143}Nd/^{144}Nd = 0{\cdot}512648$ for JMC Nd_2O_3 No. 81210. Repeated standard measurements ($n = 24$) indicate an external reproducibility (2σ) of 0·006% . For samples N7–N10 and 268–270, the initial isotopic ratios were calculated with the whole-rock–biotite isochron ages of the corresponding dykes (Table 1). For samples Oa3 and L6/1–L6/4 the initial values were calculated for an age of 445 Ma (see text). ε_{Nd} values were obtained by assuming a $^{143}Nd/^{144}Nd$ ratio of 0·512638 and a $^{147}Sm/^{144}Nd$ ratio of 0·1967 for the chondritic reservoir. Nd model ages ($T_{(DM)}$) were calculated with the depleted mantle data of Liew & Hofmann (1988): $(^{143}Nd/^{144}Nd)_{DM} = 0{\cdot}513151$, $(^{147}Sm/^{144}Nd)_{DM} = 0{\cdot}219$.

is difficult to reconcile with the regional geological evolution. Given the existence of numerous metamorphic ages in this area that are younger than 700–500 Ma, any dyke older than 700 Ma should show clear signs of metamorphic overprint. All minette samples, including those obtained from Dyke 3, show only minor signs of metamorphic alteration under greenschist-facies conditions (Hoch, 1997; Hoch & Tobschall, 1998). The dykes are furthermore undeformed and they strike almost parallel with a steep dip. Thus it is highly unlikely that

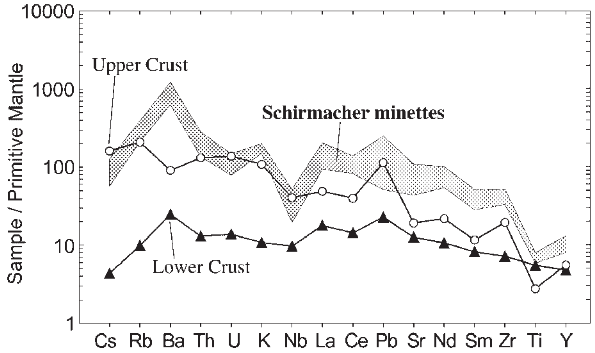

Fig. 2. Primitive mantle-normalized trace element patterns of the minette samples (Hoch & Tobschall, 1998). Average abundances for upper and lower continental crust are shown for comparison [data from Taylor & McLennan (1985)]. The primitive mantle data of Hofmann (1988) are used for normalization.

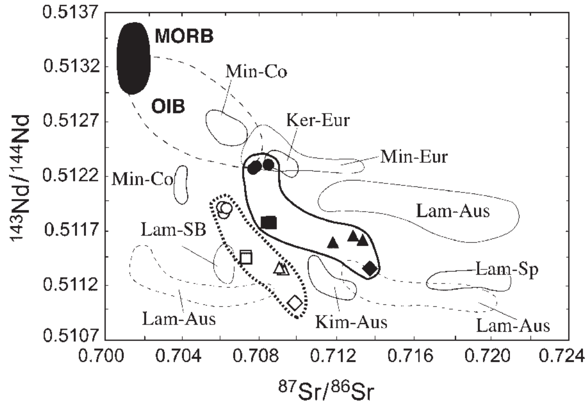

Fig. 3. Plot of $^{143}Nd/^{144}Nd$ vs $^{87}Sr/^{86}Sr$ for the Schirmacher minettes. Triangles, N7, N9, N10 (Dyke 1); squares, 268–270 (Dyke 2); circles, L6/1–L6/4 (Dyke 3); diamond, Oa3 (Dyke 4). Filled symbols are for present-day isotopic compositions; open symbols represent the initial values at time of dyke emplacement. Fields denote published data for lamprophyric rocks from other localities (data sources: McCulloch *et al.*, 1983; Fraser *et al.*, 1985; Alibert *et al.*, 1986; Nelson *et al.*, 1986; Turpin *et al.*, 1988; Thompson *et al.*, 1989; Fraser & Hawkesworth, 1992). Min, minettes; Ker, kersantites; Lam, lamproites; Kim, kimberlites; Aus, Australia; Co, Colorado; Eur, Europe; Sp, Spain; SB, Smokey Butte.

Dyke 3 was overprinted by the Pan-African orogeny, whereas Dykes 1 and 2 were unaffected by this event. This leads to the interpretation that the Rb/Sr age obtained for Dyke 3 is probably disturbed. The reason for the erroneously old age is unclear at present, but it may be due to the analysis of xenocrystic biotite, which was not in equilibrium with the host magma at the time of dyke emplacement. The good agreement in the ages of Dykes 1 and 2 with the previously published age data for lamprophyres from the Schirmacher Hills at ∼445 Ma indicates that all of the minette dykes analysed in the present study were probably emplaced at approximately the same time. For this reason, it is assumed in the following discussion that Dykes 3 and 4 were also formed at 445 Ma. It is important to note in this respect, however, that none of the conclusions that are drawn with respect to the geochemical evolution of the minette source are critically dependent upon this assumption. They would be equally valid for older eruption ages of between 445 and 750 Ma.

Sr, Nd and Pb isotopic compositions

The $^{87}Sr/^{86}Sr$ ratios of the Schirmacher minettes range from 0·7077 to 0·7134 with initial $(^{87}Sr/^{86}Sr)_i$ values of 0·7062 to 0·7102 (Table 3, Fig. 3). The Sr isotopes are thus markedly more radiogenic than would be expected for a magma derived from a 'normal' depleted upper-mantle source. Similar results are obtained for the Nd isotope compositions, with $^{143}Nd/^{144}Nd$ varying between 0·51135 and 0·51231 ($\varepsilon_{Nd} = -6·5$ to $-25·1$) and initial $^{143}Nd/^{144}Nd$ values of 0·5110–0·5119 ($\varepsilon_{Nd(t)} = -3$ to -20; Table 4, Fig. 3). The isotopic compositions of the Schirmacher minettes plot significantly below the 'mantle array' defined by mid-oceanic ridge basalts (MORB) and ocean island basalts (OIB) in a diagram of $^{143}Nd/^{144}Nd$ vs $^{87}Sr/^{86}Sr$. In this respect, the minettes are similar to many ultrapotassic rocks (e.g. lamproites, kersantites, kimberlites) from other localities worldwide (Fig. 3).

In diagrams of $^{207}Pb/^{204}Pb$ and $^{208}Pb/^{204}Pb$ vs $^{206}Pb/^{204}Pb$, the minette samples plot above and to the left of the MORB array (Fig. 4a and b, and Table 5) and above the Northern Hemisphere Reference Line (NHRL) of Hart (1984). Thus the samples are characterized by positive Δ7/4 and Δ8/4 values as defined by Hart (1984). With one exception, the present-day isotopic compositions of the samples also plot to the left of and above the 4·55 Ga geochron in Fig. 4a. It is furthermore noteworthy that the present-day and the initial Pb isotope ratios define a linear array in Fig. 4a, whereas more scatter is apparent in Fig. 4b. In both instances, however, the initial isotope ratios of the samples (which were calculated using the measured U–Th/Pb ratios of the rocks) define a tighter data cluster than the measured present-day values. This is significant, because it indicates that the U–Th/Pb systematics of the minettes was probably not significantly perturbed since dyke emplacement, for example, by recent loss of U. Clearly, minor effects of alteration cannot be ruled out at present and such effects may be responsible for the differences of initial $^{206}Pb/^{204}Pb$ ratios among the samples from Dyke 1 (Table 5, Fig. 4). In the case of Dykes 2 and 3, however, each pair of samples displays almost identical $^{206}Pb/^{204}Pb$ ratios.

In summary, the data shown in Fig. 4 are indicative of a complicated multi-stage history for the Pb isotopic evolution of the minettes: (1) the high Δ7/4 values suggest an ancient evolution of the Pb isotopes in a high-μ environment ($\mu = {}^{238}U/^{204}Pb$); (2) the relatively low

Table 5: Pb and U concentrations, Pb isotope ratios and calculated initial Pb isotope ratios of the Schirmacher minettes

Sample	Pb (ppm)	U (ppm)	$^{238}U/^{204}Pb$ (μ)	$^{206}Pb/^{204}Pb$	$(^{206}Pb/^{204}Pb)_i$	$^{207}Pb/^{204}Pb$	$(^{207}Pb/^{204}Pb)_i$	$^{208}Pb/^{204}Pb$	$(^{208}Pb/^{204}Pb)_i$
N7	34·19	2·79	5·10	17·28	16·92	15·49	15·47	38·59	37·64
N9	35·75	1·93	3·33	16·81	16·58	15·45	15·44	38·06	37·35
N10	34·92	2·04	3·61	16·77	16·52	15·46	15·45	38·14	37·50
269	12·56	2·09	10·64	18·09	17·34	15·57	15·53	39·47	37·97
270	24·08	1·63	4·22	17·52	17·22	15·54	15·53	38·37	37·54
L6/1	33·40	2·42	4·51	17·79	17·47	15·54	15·52	37·82	37·36
L6/4	43·90	2·68	3·80	17·77	17·51	15·55	15·53	37·78	37·39
Oa3	16·44	1·83	7·13	17·90	17·39	15·54	15·51	39·79	38·38

Pb isotopes are corrected for fractionation relative to the values of Catanzaro *et al.* (1968) for the NIST-981 Pb standard. The following reproducibilities (2σ, $n = 38$) were obtained for repeated measurements of NIST-981 Pb: $^{207}Pb/^{206}Pb = 0{\cdot}913999 \pm 22$ and $^{208}Pb/^{206}Pb = 2{\cdot}163470 \pm 172$. For samples N7–N10 and 268–270, the initial isotopic ratios were calculated with the whole-rock–biotite isochron ages of the corresponding dykes (Table 1). For samples Oa3 and L6/1–L6/4 the initial values were calculated for an age of 445 Ma (see text). The initial $^{208}Pb/^{204}Pb$ ratios were determined with the Th abundances of Table 1, which were obtained by inductively coupled plasma mass spectrometry (Hoch & Tobschall, 1998).

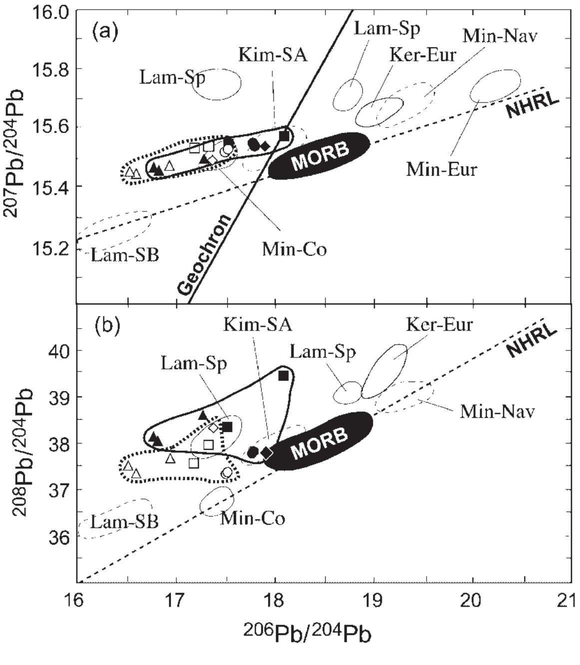

Fig. 4. Plots of (a) $^{207}Pb/^{204}Pb$ and (b) $^{208}Pb/^{204}Pb$ vs $^{206}Pb/^{204}Pb$ for minettes from the Schirmacher Oasis compared with other lamprophyric rocks and MORB. Symbols as in Fig. 3. Fields denote published data for lamprophyric rocks from other localities (see Fig. 3 for data sources and abbreviations; Nav, Navajo; SA, South Africa). NHRL, Northern Hemisphere Reference Line, from Hart (1984).

$^{206}Pb/^{204}Pb$ ratios, on the other hand, record a more recent evolution in a low-μ environment; (3) the scatter of the data in a plot of $^{208}Pb/^{204}Pb$ vs $^{206}Pb/^{204}Pb$ (Fig. 4b) is suggestive of variable time-integrated Th/U ratios.

Oxygen isotopes

The whole-rock $\delta^{18}O$ values of the Schirmacher minettes range between +6·5 and +9·5‰ (Table 6). Without exception, the minettes are thus characterized by $\delta^{18}O$ significantly higher than inferred for the upper mantle ($\delta^{18}O$ = 5·5–6‰). The observation that all minette samples are fresh, with only minor petrographic signs of alteration or overprinting by metamorphism (Hoch, 1997; Hoch & Tobschall, 1998), argues against the suggestion that the high $\delta^{18}O$ values are primarily the result of secondary alteration. Rather, the O-isotope signatures are thought to be a primary feature of the magmas. Further support for the latter interpretation is provided by the coherent initial $(^{87}Sr/^{86}Sr)_i$ ratios calculated for the minette samples of the individual dykes. If the minette samples had been strongly affected by alteration processes in the past, the calculated $(^{87}Sr/^{86}Sr)_i$ values would be expected to show more scatter than the present-day Sr isotopic compositions. Figure 3, however, indicates that this is not the case.

DISCUSSION

Evidence for crustal components in the Schirmacher minettes

The minettes from Schirmacher Oasis have a number of geochemical characteristics (e.g. high MgO, Ni and Cr abundances, *mg*-number of up to 74; Table 1) that indicate that the magmas were derived from a mantle reservoir (Hoch & Tobschall, 1998). Like other lamprophyric magmas the minettes, however, also display

Table 6: $\delta^{18}O$ values (vs SMOW) of Schirmacher minette whole-rock samples

Sample	$\delta^{18}O$ (‰)
N7	+7·8
N9	+7·1
N10	+6·5
268	+7·6
269	+7·9
270	+7·4
L6/1	+8·1
L6/2	+8·3
L6/3	+8·3
L6/4	+8·1
Oa3	+9·5

isotopic and trace element signatures that are not reconcilable with derivation of the magmas from a primitive or depleted peridotitic mantle source alone.

The Schirmacher minettes are characterized throughout by high initial $^{87}Sr/^{86}Sr$ and $^{207}Pb/^{204}Pb$ and low initial $^{143}Nd/^{144}Nd$ (Figs 3 and 4), and these results place important constraints on the time-integrated parent–daughter ratios of the isotopic systems. The data are indicative of high Rb/Sr coupled with low Sm/Nd and require an ancient high-μ environment for the development of the positive Δ7/4 values. Such signatures are diagnostic for the involvement of a component derived from the continental crust in the formation of the minette magmas. This is also in accord with the old Nd-model ages of the samples, which vary between 1·5 and 2·5 Ga (Table 4). Given that the Sm/Nd ratios of the minettes are probably similar to or higher than the respective values of the magma sources, the old model ages should record trace element fractionation events that occurred before dyke emplacement. The model ages thus indicate that the Sm–Nd systematics of the minettes is dominated by material that experienced a long time-integrated evolution in a low Sm/Nd environment, and this is likely to be continental crust. The involvement of a crustal component in magma genesis is also suggested by the oxygen isotopes, because the $\delta^{18}O$ data for the lamprophyres ($\delta^{18}O$ ~7–10) are significantly higher than depleted upper-mantle values ($\delta^{18}O$ = 5·5–6).

The trace element results obtained for the Schirmacher minettes provide further support for this interpretation. The lamprophyres are characterized by extremely high incompatible trace element abundances, and these enrichments cannot be accounted for by partial melting of a 'normal' peridotitic upper mantle. Furthermore, the trace element patterns display particularly high abundances for elements such as Rb, Ba, Pb and the LREE, combined with negative Nb and Ti anomalies (Fig. 2). It is notable that these signatures are similar, in general, to the patterns of many continental crust materials (e.g. Taylor & McLennan, 1985). The minettes furthermore have low Nb/U and Nd/Pb. With respect to these critical diagnostic ratios, the minettes thus differ significantly from oceanic basalts (which have Nb/U = 47 ± 10 and Nd/Pb = 24 ± 5) but are very similar to continental crust, which is characterized by Nb/U ~ 10 and Nd/Pb ~ 5 (Hofmann et al., 1986).

Taken together, these results clearly indicate that the geochemistry of the minettes records the involvement of a crustal component in magma genesis and there are two obvious interpretations of this observation. (1) It is conceivable that the enriched trace element and isotopic signatures of the Schirmacher minettes were produced by the contamination of depleted, mantle-derived magmas with material derived from the upper and/or lower continental crust during dyke emplacement. (2) A number of previous studies have suggested that lamprophyres are produced by partial melting of an enriched mantle reservoir characterized by high LILE and LREE concentrations. The occurrences of many calc-alkaline lamprophyres are associated with continental collision events, whereas others are related to arc environments (e.g. Foley *et al.*, 1987). In both cases continental material (either bulk crust or sediments) is recycled back into the mantle. Metasomatic agents derived from such materials are expected to be enriched in incompatible elements and could account for the formation of enriched lithospheric mantle reservoirs. The isotope and trace element data obtained for the Schirmacher minettes are used in the following to constrain the origin of the crustal signatures detected in the magmas.

Crustal contamination of magmas or contamination of the mantle source?

The minettes have significantly higher trace element abundances than average upper continental crust, with respect to most of the incompatible trace elements plotted in Fig. 2. In comparison with abundance estimates for the lower continental crust, the lamprophyres from the Schirmacher Oasis display incompatible element concentrations that are higher by a factor of ~100 for some elements (e.g. Ba, Rb; Fig. 2). This clearly indicates that bulk contamination of the depleted magmas with upper- or lower-crustal material cannot account for the enriched trace element signatures of the samples.

It is also possible that the minette magmas were contaminated by highly enriched partial melts derived from crustal material, as a result of heating of the wall rocks during dyke emplacement, and the incorporation of such melts could account for the high incompatible trace element abundances. The unradiogenic initial $^{206}Pb/^{204}Pb$ isotope ratios of some of the minettes, however, are not consistent with the assimilation of large amounts of upper-crustal material. Compared with the upper mantle, upper continental crust is generally characterized by high $^{206}Pb/^{204}Pb$, combined with high $^{87}Sr/^{86}Sr$ and low $^{143}Nd/^{144}Nd$. Therefore, contamination of a mantle-derived magma by upper crust should generate mixing curves that display increasing $^{206}Pb/^{204}Pb$ correlated with increasing $^{87}Sr/^{86}Sr$ and decreasing $^{143}Nd/^{144}Nd$. The initial isotopic ratios of the minettes define trends with different systematics, however (Fig. 5). A comparison of the initial isotope data of the minettes at 445 Ma with the isotopic compositions of possible mantle endmembers, such as depleted mantle (DM) or primitive mantle (BSE; bulk silicate Earth), furthermore indicates that the crustal contaminant would need to display low $^{206}Pb/^{204}Pb$ (<16·5) coupled with high $^{87}Sr/^{86}Sr$ and low $^{143}Nd/^{144}Nd$ (Fig. 5). This clearly argues against the contamination of the magmas by upper-crustal material. Xenoliths from the lower crust are often characterized by unradiogenic $^{206}Pb/^{204}Pb$ ratios, coupled with high $^{87}Sr/^{86}Sr$ and low $^{143}Nd/^{144}Nd$ (e.g. Rudnick & Goldstein, 1990). Despite the low average trace element concentrations of the lower crust (Fig. 2), assimilation of enriched lower-crustal melts could thus conceivably explain the isotopic correlations of the minette dataset. However, simple mass balance calculations indicate that this would require the minette magmas to assimilate >10–50% of melt generated by low-degree partial melting (<5%) of the lower crust. Such lower-crustal melts would need to be extracted from a source volume that is significantly larger than the total volume of the erupted magmas. It is considered to be unlikely that the emplacement of the volumetrically small minette dykes is capable of initiating widespread melting of the lower crust. This conclusion is supported by the high magma ascent and cooling rates inferred for lamprophyres (Spera, 1984; Esperanca & Holloway, 1987). More complex interaction processes, such as disequilibrium melting of enriched lower-crustal phases (Becker *et al.*, 1999) are also conceivable, and it is difficult to rule out such mechanisms at present. Even such contamination processes would be expected to generate increases in $^{87}Sr/^{86}Sr$ that correlate with increasing $^{18}O/^{16}O$ and SiO_2, and decreasing MgO. Such systematic correlations are not detected in the data for minette samples that are derived from the same dyke, and hence the same parental magma (Tables 1, 4 and 6). In summary, this indicates that the addition of a metasomatic fluid or melt derived from subducted continental materials to the lithospheric mantle source of the lamprophyres provides the most straightforward explanation for the trace element and isotope composition of the Schirmacher minettes.

Geochemical evolution of the mantle source of the minettes

In the following discussion, the isotope and trace element data for the minettes are used to place constraints on the composition of the mantle source of the magmas and the materials from which the metasomatic agents were derived. To this end, we explore the implications of two evolution models.

Model 1: two-component mixing

In diagrams of Nd vs Sr isotopes and $^{206}Pb/^{204}Pb$ vs $^{207}Pb/^{204}Pb$ (Fig. 5a and b) it would appear that the isotopic compositions of the Schirmacher minettes can be readily explained by a simple two-component mixing model involving a component characterized by extremely low $^{206}Pb/^{204}Pb$ (low-6/4 component, Table 7) and a 'depleted' endmember with high $^{143}Nd/^{144}Nd$, low $^{87}Sr/^{86}Sr$ and more radiogenic $^{206}Pb/^{204}Pb$. In the simplest case, the depleted endmember may represent the composition of the ambient unmetasomatized mantle lithosphere.

If two-component mixing is to explain the observed range of magma compositions, the minette data place firm constraints on the composition of the mantle endmember. The $^{207}Pb/^{204}Pb$ ratios of the DM and most mantle compositions intermediate between DM and BSE are much lower than the $^{207}Pb/^{204}Pb$ data of the minettes (Table 7, Fig. 5b). Mantle compositions similar to BSE, however, provide a suitable endmember to explain the Sr, Nd and Pb isotope systematics of the minettes by mixing with a low-6/4 component. For such a two-component mixing model to explain the spread of the minette data in diagrams of $^{87}Sr/^{86}Sr$ and $^{143}Nd/^{144}Nd$ vs $^{206}Pb/^{204}Pb$, the low-6/4 crustal endmember is required to have very variable Sr/Pb and Nd/Pb ratios, whereas Sr/Nd would need to be relatively constant (Table 7). Such systematics is required, to generate both concave and convex mixing hyperbolas in Sr–$^{206}Pb/^{204}Pb$ and Nd–$^{206}Pb/^{204}Pb$ isotope space (Fig. 5c and d). Importantly, such a scenario is feasible only if the formation of the metasomatized mantle source of the minettes was closely associated in time with the emplacement of the dykes at $\sim$445 Ma. We arrive at this conclusion because a time difference of several 100 my between source enrichment and magmatism would be associated with significant *in situ* radiogenic decay. Therefore, the variable trace element ratios of the low-6/4 endmember would translate into variable isotopic signatures, leading to the formation of sources with distinct isotopic compositions.

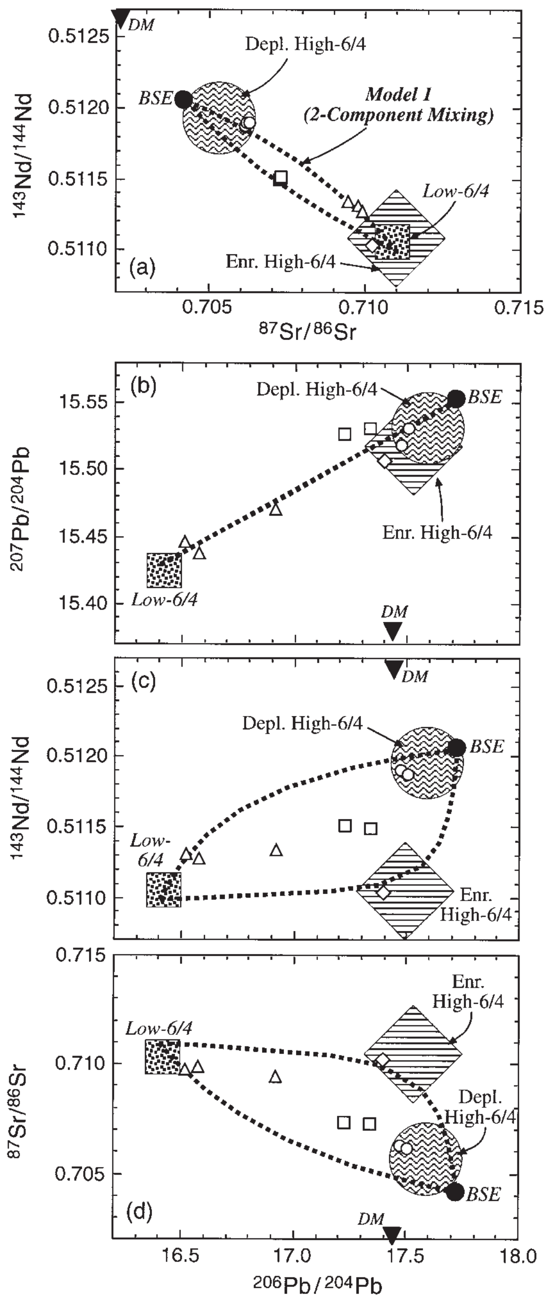

Fig. 5. Diagrams of (a) $^{143}Nd/^{144}Nd$ vs $^{87}Sr/^{86}Sr$, and (b) $^{207}Pb/^{204}Pb$, (c) $^{143}Nd/^{144}Nd$, (d) $^{87}Sr/^{86}Sr$ vs $^{206}Pb/^{204}Pb$ at 445 Ma. The systematics of the two models proposed for the geochemical evolution of the minette sources is illustrated. The various compositions are summarized in Table 7. Open symbols denote the initial isotopic compositions of the Schirmacher minettes at the time of dyke emplacement (symbols as in Fig. 3). Model 1 (with bold dashed mixing lines) is for mixing of a bulk silicate Earth (BSE) composition with a low-$^{206}Pb/^{204}Pb$ endmember characterized by variable trace element ratios. Model 2 assumes that at least three distinct compositions are required to account for the isotopic diversity of the Schirmacher minettes. These endmembers (Table 7) are indicated by the large symbols with patterns. The isotopic composition of the depleted mantle (DM) at 445 Ma (Table 7) is shown for comparison.

An obvious advantage of Model 1 is that it provides the most straightforward explanation for the almost linear trends of the minette data in Fig. 5a and b. The merits of the present model can be further evaluated by comparing the trace element ratios of the samples with those predicted by the mixing model (Fig. 6). Because of the heterogeneous trace element composition of the low-6/4 material (Table 7), the model would predict that some minettes (particularly sample Oa3) should be characterized by Sr/Pb and Nd/Pb ratios of >500 and >50, respectively (Fig. 6). Clearly, both trace element ratios can be altered during magma genesis, such that the magma compositions may not faithfully record the actual source values. The variability in Sr/Pb and Nd/Pb observed for the minettes is, however, much lower than would be predicted by the mixing hyperbolas (Fig. 6). This indicates that the present model probably does not provide a good characterization of the geochemistry of the Schirmacher minette source.

Model 2: different sources with distinct isotopic compositions

This alternative model for the evolution of the Schirmacher minette source invokes the formation of several metasomatic sources within the mantle that are characterized by distinct isotopic signatures. In the following, we focus on the three dykes with the most extreme compositions in Sr–Nd–Pb isotope space. These three dykes correspond to the following compositions (Table 7, Fig. 5): (1) a low-$^{206}Pb/^{204}Pb$ composition, with an 'enriched' geochemical signature characterized by high time-integrated Rb/Sr and low Sm/Nd (Low-6/4; Dyke 1); (2) an 'enriched' high-$^{206}Pb/^{204}Pb$ composition, displaying high time-integrated Rb/Sr and low Sm/Nd (Enr. high-6/4, Dyke 4); (3) a 'depleted' high-$^{206}Pb/^{204}Pb$ composition characterized by low time-integrated Rb/Sr and high Sm/Nd (Depl. high-6/4, Dyke 3). The identification of each dyke with a unique composition does not imply that these compositions provide a characterization of the metasomatic components that were responsible for mantle enrichment. The metasomatic agents may have displayed more extreme characteristics, but they were sampled only in diluted form or as mixtures by the minette magmas. Each of the three dykes, however, appears to be dominated by a different metasomatic component. The fourth dyke may thus represent an intermediate composition because it is a more 'balanced' mixture of the endmember components.

An advantage of Model 2 is that it does not require the existence of endmembers with 'extreme' trace element compositions (as in Model 1) that produce highly curved mixing hyperbolas in isotope space to account for the isotopic diversity of the Schirmacher minettes (Figs 5 and 6, Table 7). The Sr/Pb and Nd/Pb ratios of the

Table 7: Trace element and isotope compositions (at 445 Ma) that refer to the geochemical evolution models proposed for the mantle source of the Schirmacher minettes

		Model 1		Model 2		
	Depleted mantle (DM)	Primitive mantle/ bulk silicate Earth (BSE)	Low-$^{206}Pb/^{204}Pb$ component	Low-$^{206}Pb/^{204}Pb$ composition	Enriched high-$^{206}Pb/^{204}Pb$ composition	Depleted high-$^{206}Pb/^{204}Pb$ composition
Sr/Nd	10·1	15·3	A: 25; B: 10	~10	~10–15	~15–20
Sr/Pb	231	121	A: 50; B: 2000	~20	~100	~50–100
Nd/Pb	22·9	7·9	A: 2; B: 200	~2	~10	~5
$^{87}Sr/^{86}Sr$	0·7022	0·7042	0·7110	0·7107	0·7107	0·7060
$^{143}Nd/^{144}Nd$	0·51262	0·51206	0·51100	0·51109	0·51109	0·51200
$^{206}Pb/^{204}Pb$	17·44	17·72	16·40	16·40	17·68	17·68
$^{207}Pb/^{204}Pb$	15·38	15·55	15·43	15·42	15·55	15·55

DM, BSE: trace elements are ~10% of N-MORB abundances for DM (Rehkämper & Hofmann, 1997) and from Hofmann (1988) for BSE; isotopic compositions were calculated using either a single-stage evolution (DM: $^{87}Rb/^{86}Sr = 0{\cdot}053$, $^{147}Sm/^{144}Nd = 0{\cdot}217$; BSE: $^{87}Rb/^{86}Sr = 0{\cdot}086$, $^{147}Sm/^{144}Nd = 0{\cdot}197$; see, e.g. Rehkämper & Hofmann, 1997) or a two-stage model (DM: $\mu_1 = 0{\cdot}7$ for 4·56–4·47 Ga, $\mu_2 = 8{\cdot}75$ after 4·47 Ga; BSE: $\mu_1 = 0{\cdot}7$, $\mu_2 = 9{\cdot}05$; see, e.g. Halliday *et al.*, 1996); these parent–daughter ratios produce appropriate present-day isotopic compositions for the respective endmembers. The composition of the low-$^{206}Pb/^{204}Pb$ component of Model 1 was chosen such that two-component mixing with BSE can reproduce the range of minette compositions. The low-6/4 and the two high-6/4 compositions of Model 2 were chosen to coincide with the most extreme compositions of the minettes in Sr–Nd–Pb isotopic space (see text).

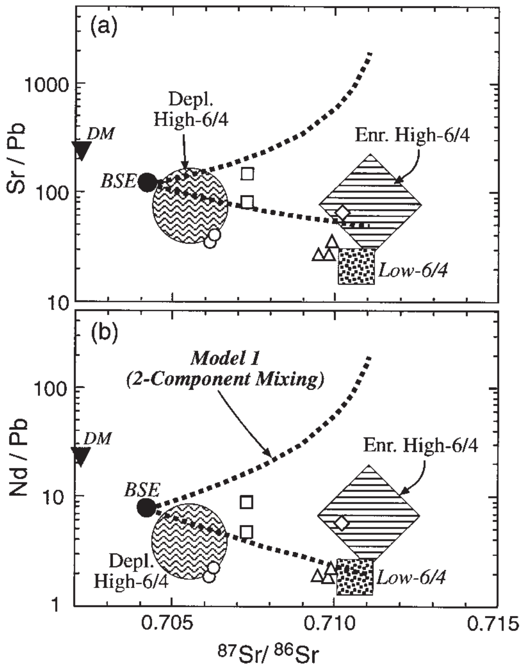

Fig. 6. Diagrams of (a) Sr/Pb and (b) Nd/Pb vs $^{87}Sr/^{86}Sr$ at 445 Ma, illustrating the consequences of the two models that are proposed for the geochemical evolution of the minette source with respect to trace element abundance ratios. All symbols as in Fig. 5. Model 1 predicts that some minette samples should display very high ratios of Sr/Pb (>1000) and Nd/Pb (>100). None of the samples, however, displays such extreme characteristics.

Schirmacher minettes display values of about 20–100 and 2–10, respectively, and such values are typical for most (continental and oceanic) crustal rocks. This indicates that the metasomatic sources of the Schirmacher minettes probably have similar characteristics and are unlikely to be characterized by the extreme trace element compositions that were inferred for the low-6/4 endmember of Model 1.

Compared with Model 1, the present scenario also places far fewer constraints on the timing of mantle source enrichment. The enrichment event may have occurred just before or significantly before dyke emplacement at 445 Ma. In the first case, the isotopic compositions of the metasomatic sources would have to be inherited directly from the metasomatic agents, which in turn were derived from the subducted material. The low-6/4 composition is most reasonably derived from the continental crust, because it is characterized by high $^{87}Sr/^{86}Sr$ and $^{207}Pb/^{204}Pb$, and low $^{143}Nd/^{144}Nd$. Such enriched isotopic signatures coupled with unradiogenic $^{206}Pb/^{204}Pb$ are rare in general, but they are a common characteristic of the lower continental crust (e.g. Rudnick & Goldstein, 1990). Incidentally, such isotopic signatures have been reported for granulite-facies rocks from Enderby Land, East Antarctica (DePaolo *et al.*, 1982). This suggests formation of the low-6/4 material by metasomatic processes involving fluids derived from lower-crustal rocks or sediments, upon subduction into the mantle. Upper-crustal material, which is typically characterized by radiogenic $^{206}Pb/^{204}Pb$, coupled with high $^{87}Sr/^{86}Sr$ and unradiogenic $^{143}Nd/^{144}Nd$, may dominate the enriched high-$^{206}Pb/^{204}Pb$ composition. The depleted high-6/4 material could either represent unmetasomatized lithospheric mantle with a BSE-like composition, or be related to a metasomatic component derived from subducted oceanic crust.

It is conceivable, however, that the enrichment of the lithospheric mantle took place several hundred million years or more before dyke emplacement, for example, in the tectonic setting of an active continental margin during the Proterozoic. In this case, a simple model age can be calculated for the formation of the low-6/4 component if it is assumed to have formed solely by retardation of *in situ* production of ^{206}Pb in low-U/Pb metasomatic materials that were derived from fluids expelled from recycled crustal rocks. This model age is obtained by estimating how long radiogenic ingrowth of ^{206}Pb must have been retarded in a low-μ environment, to account for the low $^{206}Pb/^{204}Pb$ ratios of the minettes at the time of dyke emplacement. The initial Pb isotope ratios of the metasomatic material at the time of mantle enrichment are calculated by using a two-stage Stacey–Kramers evolution (Stacey & Kramers, 1975), because this is appropriate for material ultimately derived from the upper continental crust. The samples N9 and N10 (from Dyke 1) have the most unradiogenic ^{206}Pb signatures of the present database, with $(^{206}Pb/^{204}Pb)_i$ ratios of ∼16·5–16·6 (Table 5). To generate $^{206}Pb/^{204}Pb$ isotope ratios <16·55 at 445 Ma, the enrichment event would need to have taken place at ∼1·3 Ga, given a metasomatic mantle source that displayed no further radiogenic ingrowth of ^{206}Pb as a result of a μ value of zero. For a more realistic μ value of >2, the enrichment process would need to have occurred >1·5 Ga ago. If the low-$^{206}Pb/^{204}Pb$ signatures of the minettes are thus to be explained solely by retarded *in situ* decay of ^{206}Pb in a low-U/Pb metasomatic source, this source would need to have been preserved in the mantle for a time period of ∼1 by.

If mantle enrichment occurred significantly before dyke emplacement, the isotopic tracing of the sources of the metasomatic agents is rendered difficult, if not impossible, because the trace element fractionation processes that occur during the formation of the metasomatic fluids and/or the metasomatized mantle sources are followed by significant radiogenic ingrowth. Thus, both the *in situ* radiogenic ingrowth that occurs in the minette sources and the inherited isotopic fingerprint of the metasomatic agent would play a role in defining the isotopic compositions of the minette sources at 445 Ma. The trade-off of ancient mantle enrichment, however, is the requirement that the metasomatized lithosphere is not permitted to melt for a time period of up to ∼1 by, to maintain its budget of incompatible elements. Such a scenario is conceivable, but it may be unrealistic given that the Schirmacher Oasis is not situated on a stable cratonic platform, but in a mobile belt that underwent multiple tectonic events before 445 Ma.

Ultimately, the ∼1·5 Ga model age is also applicable if the low-6/4 signatures were inherited from lower-crustal rocks during metasomatism that occurred just before the emplacement of the minette dykes. In this case, the model age, however, would 'date' crustal differentiation and the formation of a lower-crustal reservoir characterized by a low μ value. Furthermore, it should be noted that either scenario is compatible with the high $\delta^{18}O$ values of the samples. The ultimate origin of the heavy oxygen isotope signatures remains unclear, but it is likely that the high $\delta^{18}O$ values were inherited directly from the subducted rocks or sediments.

CONCLUSIONS

The Schirmacher minettes are characterized by high *mg*-number as well as high MgO, Ni and Cr abundances. This clearly indicates derivation of the magmas from a mantle source. The oxygen isotope signatures of the samples ($\delta^{18}O$ ∼7–10‰), however, are not reconcilable with the derivation of the magmas from a normal peridotitic mantle reservoir. This conclusion is further supported by the highly enriched trace element patterns and the Sr–Nd–Pb isotope systematics of samples. The geochemical characteristics of the minettes are most reasonably explained by partial melting of a lithospheric mantle source that was enriched by metasomatic components derived from recycled continental crust.

Some samples display initial $^{206}Pb/^{204}Pb$ ratios of ∼16·5 at 445 Ma, coupled with comparatively high $^{207}Pb/^{204}Pb$. This indicates the involvement of an ancient crustal component that experienced a more recent evolution a low-U/Pb environment. This could be an inherited signature of old lower-crustal material that was subducted during the Pan-African orogenic event. It is also conceivable that the mantle enrichment event pre-dated the emplacement of the minette dykes by several hundred million years. In this case, source tracing is rendered difficult, because both the *in situ* radiogenic ingrowth that occurs in the metasomatic material and its inherited isotopic fingerprint play a role in defining the isotopic composition of the minettes at the time of dyke emplacement. Which of these two factors played the dominant role will primarily be a function of the unknown timing of mantle source enrichment.

The variability of the isotopic compositions for the Schirmacher minettes is most reasonably explained by the derivation of the magmas from metasomatic sources characterized by both variable isotope and trace element compositions. Such diversity can be produced if the enriched mantle sources are formed by the addition of metasomatic fluids derived from different materials, such as upper and lower crust or pelagic and detrital sediments. Alternatively, the diversity of compositions may be related to the trace element fractionation processes that can occur during the formation of metasomatic fluids and metasomatized mantle sources. If the isotopic diversity of the Schirmacher minettes was produced solely by the recycling of upper continental crustal material, followed by trace element fractionation and variable radiogenic ingrowth, however, this would require the mantle enrichment process to have occurred >1 by before dyke emplacement. Such a scenario may be unrealistic, given that the Schirmacher Oasis is situated in a mobile belt that experienced multiple tectonic events in the past.

ACKNOWLEDGEMENTS

We thank U. Haack (Universität Gießen), S. Hoernes (Universität Bonn) and H. Köhler (Universität München) for the opportunity to use their mass spectrometry laboratories, and B. Hofmann, J. Schneider and M. Brauns for vital help with the analytical work. M.H. is grateful to U. Haack for helpful discussions, and to H. Kämpf (GeoForschungsZentrum Potsdam) for providing the minette samples. This paper benefited greatly from an informal manuscript review by K. Mezger and formal reviews by H. Becker and T. Reischmann.

REFERENCES

Alibert, C., Michard, A. & Albarède, F. (1986). Isotope and trace element geochemistry of Colorado Plateau volcanics. *Geochimica et Cosmochimica Acta* **50**, 2735–2750.

Becker, H., Wenzel, T. & Volker, F. (1999). Geochemistry of glimmerite veins in peridotites from lower Austria—implications for the origin of K-rich magmas in collision zones. *Journal of Petrology* **40**, 315–338.

Bielicki, K. H., Hiller, H. & Wand, U. (1991). A lead isotope study of pegmatitic K-feldspars from the Schirmacher Oasis, East Antarctica. *Zeitschrift für Geologische Wissenschaften* **19**, 201.

Bormann, P., Paech, H. J. & Stackebrandt, W. (1995). Conclusions on the structure, composition and history of the Earth's crust in central Queen Maud Land. In: Bormann, P. & Fritzsche, D. (eds) *The Schirmacher Oasis, Queen Maud Land, East Antarctica, and its Surroundings. Petermanns Geographische Mitteilungen Ergänzungsheft* **289**, 164–169.

Carlson, R. W. & Irving, A. J. (1994). Depletion and enrichment history of subcontinental lithospheric mantle: an Os, Sr, Nd and Pb isotopic study of ultramafic xenoliths from the northwestern Wyoming craton. *Earth and Planetary Science Letters* **126**, 457–472.

Carmichael, I. S. E., Lange, R. A. & Luhr, J. F. (1996). Quaternary minettes and associated volcanic rocks of Mascota, western Mexico: a consequence of plate extension above a subduction modified mantle wedge. *Contributions to Mineralogy and Petrology* **124**, 302–333.

Catanzaro, E. J., Murphy, T. J., Shields, W. R. & Garner, E. L. (1968). Absolute isotopic abundance of common, equal-atom, and radiogenic lead isotopic standards. *Journal of Research of the National Bureau of Standards* **72A**, 261–267.

Dayal, A. M. & Hussain, S. M. (1997). Rb–Sr ages of lamprophyre dykes from Schirmacher Oasis, Queen Maud Land, East Antarctica. *Journal of the Geological Society of India* **50**, 457–460.

DePaolo, D. J., Manton, W. I., Grew, E. S. & Halpern, M. (1982). Sm–Nd, Rb–Sr, and U–Th–Pb systematics of granulite-facies rocks from Fyfe Hills, Enderby Land, Antarctica. *Nature* **298**, 614–618.

Esperanca, S. & Holloway, J. R. (1987). On the origin of some mica-lamprophyres: experimental evidence from a mafic minette. *Contributions to Mineralogy and Petrology* **95**, 207–216.

Foley, S., Green, D. & Toscani, L. (1987). The ultrapotassic rocks: characterization, classification, and constraints for petrogenetic considerations. *Earth-Science Reviews* **24**, 81–134.

Fraser, K. J. & Hawkesworth, C. J. (1992). The petrogenesis of group 2 ultrapotassic kimberlites from Finsh Mine, South Africa. *Lithos* **28**, 327–345.

Fraser, K. J., Hawkesworth, C. J., Erlank, A. J., Mitchell, R. H. & Scott-Smith, B. H. (1985). Sr, Nd, and Pb isotope and minor element geochemistry of lamproites and kimberlites. *Earth and Planetary Science Letters* **76**, 57–70.

Grew, E. S. & Manton, W. I. (1983). Geochronological studies in East Antarctica, reconnaissance uranium/thorium/lead data from rocks in the Schirmacher Hills and Mount Stinear. *Antarctic Journal of the United States* **18**, 6–8.

Halliday, A. N., Rehkämper, M., Lee, D. C. & Yi, W. (1996). Early evolution of the Earth and Moon: new constraints from Hf–W isotope geochemistry. *Earth and Planetary Science Letters* **142**, 75–89.

Hart, S. R. (1984). A large-scale isotope anomaly in the southern hemisphere mantle. *Nature* **309**, 753–757.

Hoch, M. (1997). Geochemie und Isotopie kalkalkalischer und ultramafischer Lamprophyre aus der Schirmacher Oase und dem Wohlthatmassiv, Zentrales Queen Maud Land, Ostantarktika. Doctoral dissertation, University of Erlangen–Nuremberg, 191 pp.

Hoch, M. & Tobschall, H. J. (1998). Minettes from the Schirmacher Oasis, East Antarctica—indicators of an enriched mantle source. *Antarctic Science* **10**, 476–486.

Hofmann, A. W. (1988). Chemical differentiation of the Earth: the relationship betwen mantle, continental crust, and oceanic crust. *Earth and Planetary Science Letters* **90**, 297–314.

Hofmann, A. W., Jochum, K. P., Seufert, M. & White, W. M. (1986). Nb and Pb in oceanic basalts: new constraints on mantle evolution. *Earth and Planetary Science Letters* **79**, 33–45.

Kaiser, G. & Wand, U. (1985). K–Ar dating of basalt dykes in the Schirmacher Oasis area, Dronning Maud Land, East Antarctica. *Zeitschrift für Geologische Wissenschaften* **13**, 299–307.

Kämpf, H. & Stackebrandt, W. (1985). Crustal evolution of the eastern Antarctic craton (Schirmacher Oasis, Dronning Maud Land). *Gerlands Beiträge zur Geophysik* **94**, 251–258.

Liew, T. C. & Hofmann, A. W. (1988). Precambrian crustal components, plutonic associations, plate environment of the Hercynian Fold Belt of central Europe: indications from a Nd and Sr isotopic study. *Contributions to Mineralogy and Petrology* **98**, 129–138.

Ludwig, K. R. (1999). *Isoplot/Ex Version 2·01. Berkeley Geochronology Center Special Publication 1a*. Berkeley, CA: Berkeley Geochronology Center.

McCulloch, M. T., Jaques, A. L., Nelson, D. R. & Lewis, J. D. (1983). Nd and Sr isotopes in kimberlites and lamproites from Western Australia: an enriched mantle origin. *Nature* **301**, 400–403.

Nelson, D. R. (1992). Isotopic characteristics of potassic rocks: evidence for the involvement of subducted sediments in magma genesis. In: Peccerillo, A. & Foley S. (eds) *Potassic and Ultrapotassic Magmas and their Origin. Lithos, Special Issue* **28**, 403–420.

Nelson, D. R., McCulloch, M. T. & Sun, S. S. (1986). The origins of ultrapotassic rocks as inferred from Sr, Nd, and Pb isotopes. *Geochimica et Cosmochimica Acta* **50**, 231–245.

Paech, H. J. & Stackebrandt, W. (1995). Geology. In: Bormann, P. & Fritzsche, D. (eds) *The Schirmacher Oasis, Queen Maud Land, East Antarctica, and its Surroundings. Petermanns Geographische Mitteilungen Ergänzungsheft* **289**, 59–119.

Ravich, M. G. & Krylov, A. J. (1964). Absolute ages of rocks from East Antarctica. In: Adie, R. J. (ed.) *Antarctic Geology*. Amsterdam: North-Holland, pp. 579–589.

Ravich, M. G. & Soloviev, D. S. (1966). Geologiya i petrologiya Tsentralnoy Chasti gor zemli korolevy mod (Vostochnaya Antarktida) (in Russian). *Tom 141, Trudy Nauchno-Issledovatelskogo Instituta Geologii, Arktiki.* Leningrad: Nedra.

Rehkämper, M. & Hofmann, A. W. (1997). Recycled ocean crust and sediment in Indian Ocean MORB. *Earth and Planetary Science Letters* **147**, 93–106.

Rogers, N. W., Bachinski, S. W., Henderson, P. & Parry, S. J. (1982). Origin of potash-rich basic lamprophyres: trace element data from Arizona minettes. *Earth and Planetary Science Letters* **57**, 305–312.

Rudnick, R. L. (1995). Making continental crust. *Nature* **378**, 571–578.

Rudnick, R. L. & Goldstein, S. L. (1990). The Pb isotopic composition of lower crustal xenoliths and the evolution of lower crustal Pb. *Earth and Planetary Science Letters* **98**, 192–207.

Sengupta, S. (1988). Precambrian rocks of the Schirmacher Range, East Antarctica. *Zeitschrift für Geologische Wissenschaften* **16**, 647–660.

Sengupta, S. (1991). Structural and petrological evolution of basement rocks in the Schirmacher Hills, Queen Maud Land, East Antarctica. In: Thomson, M. R. A., Crame, J. A. & Thomson, J. W. (eds) *Geological Evolution of Antarctica*. Cambridge: Cambridge University Press, pp. 95–97.

Spera, F. J. (1984). Carbon dioxide in petrogenesis, III. Role of volatiles in the ascent of alkaline magma with special reference to xenolith-bearing mafic lavas. *Contributions to Mineralogy and Petrology* **88**, 217–232.

Stacey, J. S. & Kramers, J. D. (1975). Approximation of terrestrial lead isotope evolution by a two-stage model. *Earth and Planetary Science Letters* **26**, 207–221.

Stern, R. A. & Hanson, G. N. (1992). Origin of Archaean lamprophyre dykes, Superior Province, Canada: rare earth element and Nd–Sr isotopic evidence. *Contributions to Mineralogy and Petrology* **111**, 515–526.

Stille, P., Oberhänsli, R. & Wenger-Schwenk, K. (1989). Hf–Nd isotopic and trace element constraints on the genesis of alkaline and calc-alkaline lamprophyres. *Earth and Planetary Science Letters* **96**, 209–219.

Taylor, S. R. & McLennan, S. M. (1985). *The Continental Crust: its Composition and Evolution*. Oxford: Blackwell Scientific, 312 pp.

Thompson, R. N., Leat, P. T., Dickin, A. P., Morrison, M. A., Hendry, G. L. & Gibson, S. A. (1989). Strongly potassic mafic magmas from lithospheric sources during continental extension and heating: evidence from Miocene minettes of northwest Colorado, USA. *Earth and Planetary Science Letters* **98**, 139–153.

Turpin, L., Velde, D. & Pinte, G. (1988). Geochemical comparison between minettes and kersantites from the western European Hercynian orogen: trace element and Pb–Sr–Nd isotope constraints on their origin. *Earth and Planetary Science Letters* **87**, 73–86.

Wand, U., Geisler, M. & Korich, D. (1988). Petrography and geochemistry of lamprophyres from the Schirmacher Oasis, Dronning Maud Land, East Antarctica. *Zentralinstitut für Isotopen—und Strahlenforschung Leipzig—Mitteilungen* **143**, 123–124.

Wyman, D. A. & Kerrich, R. (1993). Archean shoshonitic lamprophyres of the Abitibi Subprovince, Canada: petrogenesis, age, and tectonic setting. *Journal of Petrology* **34**, 1067–1109.